

Automatic cerebral magnetic resonance image segmentation using artificial neural network

Nahid Khamisi nasab

Department of Electrical Engineering, Faculty of
Engineering
Kazerun Branch, Islamic Azad University
Kazerun, Iran
nkhn67@yahoo.com

Mohammad hosein Fatehi

Department of Electrical Engineering, Faculty of
Engineering
Kazerun Branch, Islamic Azad University
Kazerun, Iran
Mh_fatehi@yahoo.com

Abstract—Nowadays, Magnetic Resonance Imaging (MRI) is used in various fields of study and diagnosis of brain's structures and tissues. Image zoning is one of the fundamental phases in vision systems of machine. Due to adverse factors such as noise, low contrast and heterogeneity intensity of MRI images and based on high volume of information, manual zoning is considered a time-consuming and complex task. Therefore, we need automatic techniques for zoning images to analyse the tissues and structures of brain. In this study, segmentation has been presented based on multilayer perceptron neural network. The suggested method has three main phases including a) pre-processing: improving the brightness and removal of non-brain tissue, b) feature extraction: extraction of both statistical and non-statistical characteristics of each voxel and c) classification: assigning each voxel using a three-layer perceptron neural network in one of the classes of GM, WM and CSF. The qualitative and quantitative results showed the accuracy and efficiency of the proposed algorithm compared with conventional zoning methods.

Keywords: MRI; image zoning; artificial neuronal network; multilayer perceptron.

I. INTRODUCTION

The improvement of imaging technology results in accurate and good quality imaging of internal human organs such as brain. All these images play an important role in different medical fields such as injury detection and evaluation, preparation and conduct of operations and statistical studies. Given the current imaging techniques, Magnetic Resonance Imaging has a sublime place because the MRI images are embedded with appropriate spatial and high resolution of tissues. This method, as a diagnostic modality, is widely used for illustrating, analyzing and studying the anatomy of disease and malformation, identifying tumors and assisting complicated operations.

II. BRAIN STRUCTURE

Brain is covered with a grey layer called Grey Matter (GM) and there is a mass white layer beneath it, called White Matter (WM). Although brain is

protected with a skull bone layer, Cerebrospinal Fluid (CSF) has been also designated for better protection and nourishing. Brain's grey matter is the most important and fundamental part of central nervous system which contains nervous cell's body and also dendrites and axons with or without myelin. The white matter has a white colour due to high volume of fat. White matter contains the axons which connect the grey areas that actually have the nervous signals. Cerebral fluid is similar to blood plasma and the main food resource for brain. In Figure.1, three tissue types of brain have been shown.



Fig. 1. Main brain tissues: A) Main image. B) GM. C) CSF. D) WM

A B C D

III. REVIEWING THE ZONING METHODS OF MRI BRAIN IMAGES OF

The zoning methods can be divided in three groups: 1- user-centered methods, 2- semi-automatic methods and 3- fully-automatic methods.

User-centered methods are the basic and the nethermost generations of processing methods which include low level and user centered techniques. Some of these methods are thres holding techniques, regional growth, combining and separation the areas and edge detection.

The second generations used the methods which make the user role less apparent and move toward automation. In this generation, some methods including uncertainty models, optimization methods, statistical pattern recognition, clustering, forming models, artificial neural networks and Markov model are used.

The third generation contains the fully automatic with high accuracy methods. In these techniques, the high level information such as background data, defined rules by experts and formative models are used. Such methods are Atlas-based methods, law-based procedures and formative models.

IV. METHODS BASED ON ARTIFICIAL NEURAL NETWORK

Artificial Neural Networks (ANN) is simple models of real nervous systems from which the complexity will be removed while modeling.

In a simple view, a nerve model includes entrances which are multiplied in weights, to determine the signal strength. Finally, a math solution will determine whether neurons are active or not and if the answer is positive, outputs will be specified.

In 2000, Constentino used Som neural network in order to zone the skull in MRI images and brightness feature was used for network training [1]. Figure. 2 show a neuron picture and its mathematical model:

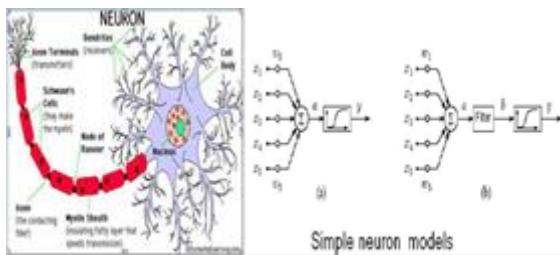


Fig. 2. A neuron picture and its mathematical model. A) Real model. B) Mathematical model

Learning Vector Quantization (LVQ) is another network of zoning images. This method is a clustering technique in which every output neuron represents a specific group of models. In these networks, output neurons' position is verified by monitoring their weight through education in the educational process, which results in approximate decision pages of classification [2].

Third and most used network which is indicated in issues such as: compression, function approximation, classification and images zoning, is the Multilayer Perceptron (MLP) [3] which will be described in details in method and material section.

Magnotta et al (1999) used intensity value of voxels (IIVs) as image features and zoned MRI images with high resolution [4].

Powell et al (2008) developed Magnotta algorithm and in addition of IIVs, they used a probability map for zoning the brain structures in high resolution images [5].

Jabarouti Moghadam et al (2009) used the IIVs and voxel spatial coordinates and GMIs geometric variables to improve the distinction between brain structures in MRI images.

V. FSL SOFTWARE

FSL is one of the most functional brain analysis software which has been presented by FMRIB Analysis Group. This application contains different modules such as BET for extracting brain and FAST for zoning tissues and FILTER for synchronization.

VI. MATERIALS AND METHODS

In the proposed algorithm, the first stage is pre-processing which includes skull removal, correction of heterogeneity of image intensity and improvement of image brightness. The second stage is extracting statistical and non-statistical features of images. The last stage is zoning images based on multilayer perceptron neural network to three tissues of GM, WM and CSF. Image (3) shows the proposed algorithm including the three steps listed above.

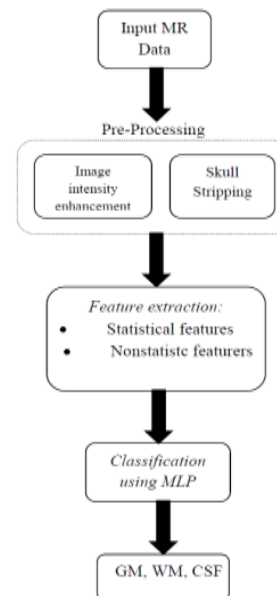


Fig. 3. Diagram block of proposed algorithm

VII. PRE-PROCESSING

In this step, zoning on entrance images is used in order to decrease artifacts such as noise and heterogeneity of intensity and enhancement of accuracy. The latter includes skull removal and improvement of intensity. In this study, FSL is used for improving heterogeneity of intensity. Also, histogram matching method is used to improve contrast. Figure 5 and figure 6 indicate this process.

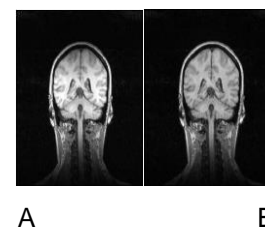


Fig. 4. Improvement of heterogeneity of intensity using FSL. A) Real picture B) Improved picture.

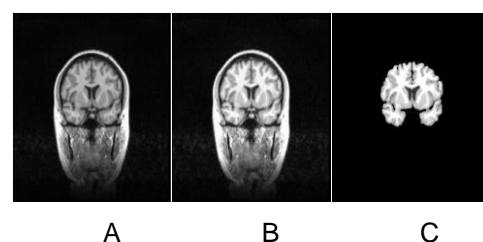


Fig. 5. The picture with improvement of heterogeneity. A) The picture with contrast improvement, B) Removal of skull in picture (picture are obtained from IBSR)

$$\text{Correlation} = \sum_x \sum_y (x - \mu_x)(y - \mu_y) \frac{I(x,y)}{\sigma_x \sigma_y} \quad (6)$$

$$\mu_x = \sum_x \sum_y x I(x,y) \quad (7)$$

$$\sigma_x = \sum_x \sum_y (x - \mu_x)^2 I(x,y) \quad (8)$$

VIII. FEATURE EXTRACTION

ASTATISTICAL CHARACTERISTIC (GREY MATTER)

In medical image processing, three-dimensional data $M*N*L$ with grey matter are assumed as $M*N*L$ matrix. This matrix can represent a method in four-dimensional area, in which every voxel or element of this matrix with x, y, z will have I grey matter. Intensity, mean, median and standard variance are characters of grey matter which have been reviewed in this study. Mean and variance are described as following.

$$m = \frac{1}{x+y+z} \sum_x \sum_y \sum_z I(x,y,z) \quad (1)$$

$$\text{std} = \frac{1}{x+y+z} \sum_x \sum_y \sum_z (I(x,y,z) - m)^2 \quad (2)$$

a) TISSUE CHARACTERISTICS

Tissue characteristics are described as repeating on or more model in one area and are the second order of statistical characteristics through which the differences between grey matters of two pixels in different location will be compared. Energy, entropy, contrast and correlation are the features which have been examined in this study.

Energy: this quantity is a measure for image homogeneity. This measure is a good criterion for detecting the difference and irregularities in the image. The higher quantity of measure means the intensity has fewer changes in the image.

$$m = \frac{1}{x+y+z} \sum_x \sum_y \sum_z I(x,y,z) \quad (3)$$

Contrast: it is another measurement which indicates the local changes in image. The greater quantity in contrast means high local changes which results in an image with better resolution.

$$\text{Contrast} = \sum_x \sum_y (x - y)^2 I(x,y) \quad (4)$$

Entropy: as a statistical characteristic of image, entropy is a measurement for modification, which can represent one of the features of tissue.

$$\text{Entropy} = \sum_x \sum_y I(x,y) \text{Log}(I(x,y)) \quad (5)$$

Correlation: based on the following equation, in a random image, the value of correlation is approximately zero.

b) NON-STATISTICAL CHARACTERISTIC

Geometric torque of $(p+q+r)$ in image (z,x,y,z) is calculated with the following equation in which M,N,L are the image dimensions. In this study, first, second and third orders torque were used.

$$m_{pqr} = \sum_{x=0}^{M-1} \sum_{y=0}^{N-1} \sum_{z=0}^{L-1} x^p y^q z^r I(x,y,z), p, q, r = 1, 2, \dots \quad (9)$$

IX. IMAGE ZONING BY NEURAL NETWORK

After extracting 21 feature from each voxel, the last step is zoning an image for determining class (group) of each voxel. In this stage, each voxel is assigned to one of the groups of GM, WM or CSF. In this study, a three-layered perceptron neural network with 50 neurons in hidden layer and propagation's educational algorithm was used.

X. MULTILAYER PERCEPTRON

The multilayer perceptron has one input layer, one or more hidden layers and one output layer. In this structure, all one layered neurons are attached to the neurons of next layer. Figure.6 illustrate one perceptron network. The number of neurons in each layer is separated from the number of neurons in other layers.

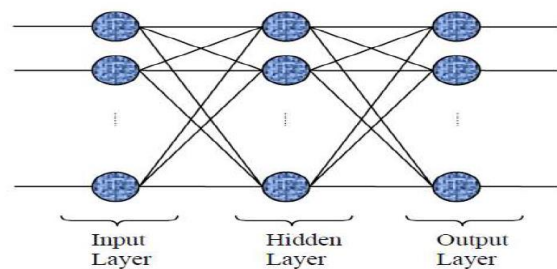


Fig. 6. Three layered perceptron model

In the above image, each circle performs operation and threshold. Output of i^{th} neuron in last layer can be shown as following.

$$o_i = \text{sgm} \left(\sum_m \text{sgm} \left(\sum_l x_l w_{lm}^h \right) w_{mi}^o \right) \quad (10)$$

In which,

O and h indicate output and hidden layers, respectively, and

W is the weight of layers.

Sgm is also sigmoid function which can be defined as follow:

$$sgm = \frac{1}{1 + e^{-x}} \quad (11)$$

XI. NETWORK TRAINING

Generally, artificial neural networks are divided to two groups of fixed weight and variable weight or learner. Learning networks are also divided to two groups of supervised or unsupervised. In supervised networks, in training phase, the sample with known ideal corresponding is used. On the other words, input samples have sign. In unsupervised networks, based on a measure, as an example distance and due to output competition, they will organize in different groups. In order to train network and modify weight to achieve a significant error, there is various ways. One of the most famous methods is propagation algorithm.

c) TISSUE CHARACTERISTICS

This algorithm can be used for forward neural networks. In forward neural networks, neurons are placed in successive layers and set their output forward. Propagation means errors are fed backwards in order to modify weights and after that, they repeat the input path to output. In this algorithm, it is assumed that the network's weights are chosen randomly. In each step, output is compared with ideal output and based on the differences of these two outputs; weights will be modified to decrease the error.

XII. NETWORK TRAINING

In order to evaluate the zoning method and its use in proposed algorithm, four common criteria are used: The Dice coefficient, Jaccard coefficient which is similar criteria, and sensitivity and specificity which success and error rate criteria are

d) DICE COEFFICIENT

Dice coefficient or similarity index represents spatial overlap between two binary images. It has the amount of zero (without overlap) and one (maximum overlap).

$$D(T, S) = \frac{2|T \cap S|}{(|T| + |S|)} = \frac{2|TP|}{(|TP| + |FN| + |TN| + |FP|)} \quad (12)$$

e) JACCARD COEFFICIENT

It is another common measurement for determining the similarity between the automatic segmented image and manual segmented image.

$$J(T, S) = \frac{|T \cap S|}{|T \cup S|} = \frac{|TP|}{(|TP| + |FN| + |FP|)} \quad (13)$$

f) SUCCESS AND ERROR RATE CRITERIA

Insensitivity or True Positive Factor (TPF) refers to the ability to identify the right tissue in segmented mask.

$$TPF = \frac{TP}{TP + FN} \quad (14)$$

Feature or true negative factor (TNF) refers to the ability of zoning in right elimination of undesirable voxels.

$$TNF = \frac{TN}{TN + FP} \quad (15)$$

If X is the voxels of image and $T \in X$ are the results of zoning and $S \in X$ are the assessing results, true positive (TP) shows the number of voxels which have been chosen rightly in assumed group, false negative (FN) shows the number of voxels which have been chosen wrongly in assumed group, false positive shows the number of voxels which have been chosen wrongly in assumed group and true negative (TN) shows the number of voxels which have been chosen rightly in non-assumed group.

XIII. BRAIN MRI DATA

For measuring represented algorithm, simulated data from Brain web database and real data from IBSR have been used in this study.

g) SIMULATED DATA FROM BRAIN WEB

Three dimension simulated images in this database have voxel in $181 \times 217 \times 181$ and resolution of 1 millimeter cubes. This database produces simulated realistic data with non-uniform level of intensity resulting from RF with noise. Also, the reference images corresponding with above image is available in this database.

h) IBSR REAL DATA

These data contain 20 normal samples of brain MRI which have been collected from morph metric analysis centre at Massachusetts General Hospital. Brain MRI data and zoning results are available by experts in this center. Furthermore, IBRS provided the results of 5 automatic zoning methods by which comparison of measured results with other common methods is offered.

XIV. BRAIN MRI DATA

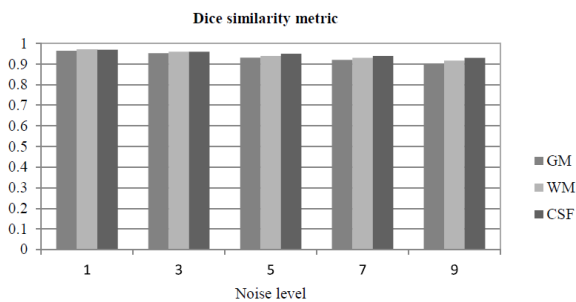
the results for zoning of Brain web simulated images among the T1 images of Brain web database, image without noise and RF image for training neural network has been considered. This job has been done by extracting 21 features of each voxel and use of three layered perceptron neural network and propagation algorithm.

In order to asses, images with different noise and RF were examined. First, using the FSL application, images' heterogeneity was corrected and skull removal was done with BET module. Then, by

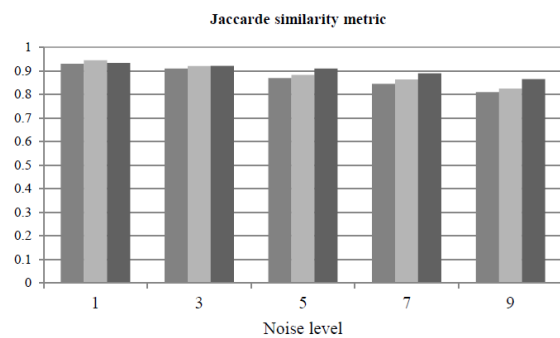
extracting 21 features of images and by using trained networks' weights, image zoning was done. Table (1) and Figure 7 show the bar graph of results. And Figures 8 and 9 shows zoning on images with 3, 5 and 7% noise.

TABLE I. Evaluating proposed method on Brain web images based on Dice and Jaccard standard.

Noise level	Dice			Jaccard		
	GM	WM	CSF	GM	WM	CSF
1	0.970	0.960	0.970	0.945	0.931	0.933
3	0.960	0.950	0.960	0.921	0.910	0.922
5	0.940	0.930	0.950	0.883	0.870	0.910
7	0.930	0.920	0.940	0.864	0.845	0.890
9	0.900	0.890	0.930	0.815	0.800	0.860



A



B

Fig. 7. Bar graph of proposed method of Brain web images based on A) Dice standard B) Jaccard standard

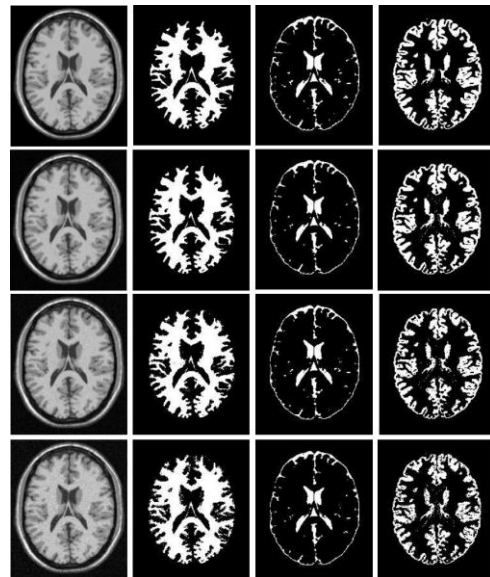


Fig. 8. Zoning of 90 axial cutting T1 images with 3, 5 and 7 % noise from Brain web database

XV. THE RESULTS FROM IBRS REAL IMAGES' ZONING

Since these data are the results of real imaging, some issues such as small brain volume, sudden changes in light intensity, high heterogeneity and noise as negative factors are included in zoning. Table 2 indicates quantitative results for IBRS data based on simulated Dice and Jaccard coefficient. In order to better understanding of results of figure.8, bar graph has been provided in figure.9.

TABLE II. Evaluation of proposed method on IBRS images based on Dice and Jaccard standard.

Image	Dice			Jaccard		
	GM	WM	CSF	GM	WM	CSF
100_23	0.920	0.866	0.441	0.851	0.764	0.283
205_3	0.836	0.825	0.544	0.718	0.702	0.373
202_3	0.906	0.862	0.608	0.828	0.758	0.436
191_3	0.864	0.838	0.328	0.760	0.721	0.196
110_3	0.864	0.828	0.108	0.760	0.708	0.057
17_3	0.853	0.836	0.272	0.744	0.718	0.158
16_3	0.761	0.760	0.301	0.614	0.613	0.177
15_3	0.817	0.777	0.367	0.690	0.635	0.225
13_3	0.908	0.868	0.419	0.832	0.767	0.265
12_3	0.864	0.826	0.599	0.760	0.704	0.427
11_3	0.865	0.825	0.551	0.762	0.703	0.381
8_4	0.839	0.823	0.305	0.722	0.699	0.180
7_8	0.831	0.836	0.256	0.710	0.718	0.147
6_10	0.799	0.745	0.284	0.665	0.594	0.165
5_8	0.812	0.737	0.375	0.683	0.583	0.230
2_4	0.861	0.819	0.327	0.756	0.693	0.196
4_8	0.846	0.797	0.346	0.733	0.663	0.209
111_3	0.845	0.829	0.429	0.732	0.706	0.273
112_2	0.883	0.855	0.194	0.790	0.747	0.108
Average	0.850	0.819	0.371	0.743	0.695	0.236

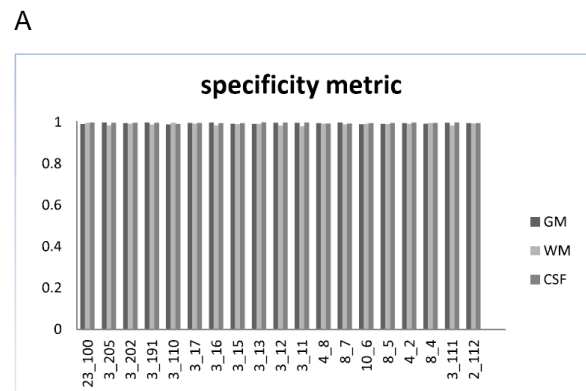
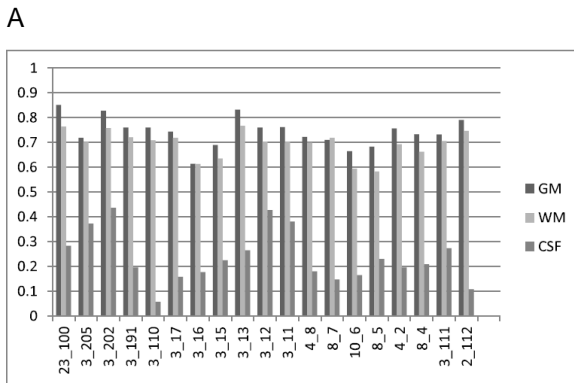
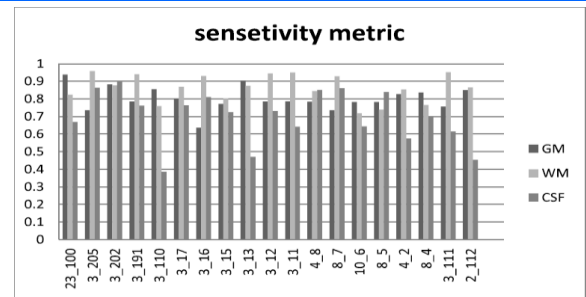
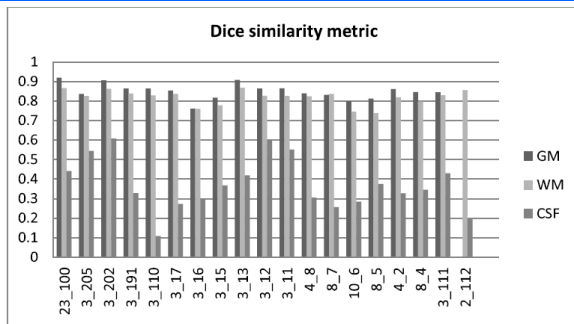


Fig. 9. Bar graph of proposed method on IBRS images based on A) Dice standard, B) Jaccard standard

Based on obtained results from table, if the noise and heterogeneity was high, in a way that image noise and heterogeneity cannot be brought to an acceptable level by pre-processing, poor results are obtained from similarity measurement.

In the following, for more measurement of proposed method, the results of success and failure rates' criteria are shown in Table (3) and bar graph of figure.10.

TABLE III. Evaluation of proposed method on IBRS images based on sensitivity and feature measurement

Image	sensitivity			specificity		
	GM	WM	CSF	GM	WM	CSF
100_23	0.938	0.823	0.668	0.991	0.996	0.998
205_3	0.735	0.957	0.863	0.998	0.984	0.997
202_3	0.882	0.877	0.897	0.995	0.993	0.997
191_3	0.785	0.940	0.761	0.998	0.988	0.997
110_3	0.856	0.758	0.386	0.989	0.997	0.992
17_3	0.801	0.868	0.763	0.996	0.993	0.996
16_3	0.636	0.930	0.810	0.998	0.984	0.995
15_3	0.771	0.803	0.724	0.993	0.990	0.995
13-3	0.903	0.874	0.470	0.992	0.992	0.999
12_3	0.785	0.945	0.731	0.997	0.983	0.998
11_3	0.786	0.950	0.642	0.997	0.980	0.998
8_4	0.784	0.845	0.851	0.995	0.993	0.994
7_8	0.735	0.928	0.860	0.998	0.990	0.994
6_10	0.782	0.718	0.644	0.990	0.992	0.995
5_8	0.782	0.739	0.839	0.992	0.991	0.996
2_4	0.827	0.854	0.575	0.995	0.992	0.998
4_8	0.836	0.765	0.702	0.993	0.995	0.996
111-3	0.756	0.952	0.614	0.997	0.983	0.998
112_2	0.850	0.865	0.454	0.995	0.994	0.995
Average	0.802	0.863	0.698	0.995	0.990	0.996

Fig. 10. Bar graph of proposed method on IBRS images base on A) sensitivity B) feature

As it can be observed from table 3, the mean of feature measurement for 19 figures of GM, WM and CSF tissues are 99.5%, 99% and 99.6% respectively. These results indicate that presented algorithm has great ability in removing undesirable areas and voxels in intended tissue. In Table (4) the represented method is compared with some other common methods.

TABLE IV. Comparison of proposed method with other common methods

Methods	Gray matter	White matter
Manual (4 brains averaged over 2 experts)	0.876	0.832
Proposed method	0.743	0.695
adaptive MAP	0.564	0.567
biased MAP	0.558	0.562
fuzzy c-means	0.473	0.567
Maximum A posteriori Probability (MAP)	0.55	0.554
Maximum-Likelihood	0.535	0.551
tree-structure k-means	0.477	0.571
MPM-MAP	0.683	0.662
FSL-FAST	0.611	0.634
SPM	0.652	0.670

Presented results in Table (4) shows that the proposed method has better results comparing to other reported method. It can be indicated that proposed algorithm has similar results to expert zoning both for segmentation of GM and WM.

Reference

[1] Reyes-Aldasoro CC, Aldeco AL. Image segmentation and compression using neural networks. Advances in Artificial Perception and Robotics CIMAT. 2000 Oct. 23-5.

[2] Yang MS, Lin KC, Liu HC, Lirng JF. Magnetic resonance imaging segmentation techniques using batch-type learning vector quantization algorithms. *Magnetic resonance imaging*. 2007 Feb 28;25(2):265-77.

[3] Miller AS, Blott BH. Review of neural network applications in medical imaging and signal processing. *Medical and Biological Engineering and Computing*. 1992 Sep 1; 30(5):449-64.

[4] Magnotta VA, Heckel D, Andreasen NC, Cizadlo T, Corson PW, Ehrhardt JC, Yuh WT. Measurement of brain structures with artificial neural networks: Two-and three-dimensional applications 1. *Radiology*. 1999 Jun; 211(3):781-90.

[5] Powell S, Magnotta VA, Johnson H, Jammalamadaka VK, Pierson R, Andreasen NC. Registration and machine learning-based automated segmentation of subcortical and cerebellar brain structures. *Neuroimage*. 2008 Jan 1; 39(1):238-47.

[6] JabaroutiMoghaddam M, Rahmani R, Soltanian-Zadeh H. Automatic segmentation of putamen using geometric moment invariants. In the 15th Iranian Conference on Biomedical Engineering, Mashad, Iran 2009.

[7] Dice LR. Measures of the amount of ecologic association between species. *Ecology*. 1945 Jul 1; 26(3):297-302.

[8] Jaccard P. The distribution of the flora in the alpine zone. *New phytologist*. 1912 Feb 1; 11(2):37-50.